SEMARAK ILMU PUBLISHING

Journal of Advanced Research in Fluid Mechanics and Thermal Sciences

Journal homepage:
https://semarakilmu.com.my/journals/index.php/fluid_mechanics_thermal_sciences/index
ISSN: 2289-7879

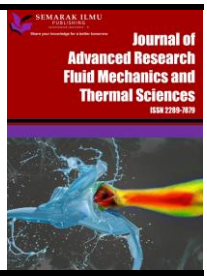

Effects of Electroosmosis on Peristaltic Flow of Eyring-Powell Fluid through a Non-Uniform channel: An Application to Blood flow

Anoop Naduvathedath Kizhakkumpatt[1], Manjunatha Gudekote[1,*], Rajashekhar Vitthal Choudhari[2], Hanumesh Vaidya[3], Kerehalli Vinayaka Prasad[3], Kuppalapalle Vajravelu[4]

[1] Department of Mathematics, Manipal Institute of Technology, Manipal Academy of Higher Education, Manipal, India
[2] Department of Mathematics, Manipal Institute of Technology Bengaluru, Manipal Academy of Higher Education, Manipal, India
[3] Department of Mathematics, Vijayanagara Sri Krishnadevaraya University, Ballari, Karnataka, India
[4] Department of Mathematics, University of Central Florida, Orlando, FL 32816, United States

ARTICLE INFO

Article history:
Received 21 May 2024
Received in revised form 26 September 2024
Accepted 5 October 2024
Available online 20 October 2024

Keywords:
Electroosmosis; Eyring-Powell fluid; varying viscosity; perturbation

ABSTRACT

This study examines the electroosmotic effects of a non-uniform passage during the peristaltic phase of an Eyring-Powell model fluid. Understanding how the channel walls affect fluid flow issues in biofluid dynamics is the main goal of the study. Integrating the convective boundary conditions into the series perturbation paradigm is the main focus of the work, assuming low Reynolds number and a long wavelength. For temperature, velocity, stream function and concentration, the governing non-linear equations have their solutions found. MATLAB R2023a software is used to demonstrate a graphical presentation of the study's improvements in accessibility through parametric assessment. The research yields important insights, particularly regarding natural phenomena like blood flow in small arteries, which might be utilized for intervention or management in dysfunctional circumstances. As the analysis demonstrates, different viscosities also have a big role in boosting the temperature profiles, and electroosmotic parameters have a major impact on the fluid properties.

1. Introduction

The study of fluid motion that often alternates between narrowing and relaxing is known as the peristaltic process. As the flow continues, the transport medium's volume varies. The peristaltic mechanism's analysis and mathematical modelling have produced several intriguing elements for academics. The applications that have been found fall into the industrial and biological categories. Industrial personnel benefit from the peristaltic motion because the contraction and relaxation control the flow speed, lowering the need for an external force to control the flow. Beginning with Latham [1], the study of peristalsis involved modelling the transport of urine across the ureter, which revolutionized the modelling of peristaltic transport. The concept was then redesigned by Shapiro *et al.,* [2] utilising the low Reynolds number and long wavelength assumptions. Many studies have been

* *Corresponding author.*
E-mail address: manjunatha.g@manipal.edu

https://doi.org/10.37934/arfmts.122.2.156180

steered using the Newtonian model fluid to analyse the peristaltic transport; nevertheless, it is possible that some processes do not adhere to the Newtonian principles of viscosity, such as the passage of urine across the ureter, faeces transiting the gastrointestinal zone, and food bolus going through the oesophagus. The first people to mathematically simulate non-Newtonian fluid flow were Raju and Devanathan [3]. Numerous researchers pursued the concept to investigate different aspects. Srivastava *et al.,* [4] examined the power-law fluid as a non-Newtonian model, applying the shape of the flow medium and contrasting the uniform and non-uniform channel effects. Misra and Pandey [5] investigated the impact of peristalsis on physiological fluids and found that higher fluid behaviour indices and thinner peripheral layers can both result in higher flow rates. Using a combination of profiles, Hariharan *et al.,* [6] modelled both the Bingham fluid model and the Power Law, solved the model using Fourier series expansions, and determined how the amplitude ratio and power law index affected the pressure increase.

Two examples of the many areas in which peristaltic flow with heat and mass transport are relevant are heat convection from blood flow via tissue pores and conduction within tissues. The control of body temperature throughout the entire body is one of the primary roles of the human circulatory system. The effect that heats transfer has on the flow must be considered while analysing the flow characteristics. Temperature differences allow one form of energy to transcend boundaries: heat. When peristaltic transport and heat transfer are considered, oxygenation and haemodialysis have also been seen. Peristaltic heat transfer has extensive uses in energy transmission in wet chilling towers, evaporation on the water body surfaces, and drying processes. Reverse osmosis, membrane separation, distillation, combustion, and diffusion of chemical pollutants are just a few industrial processes that involve mass transfer. By packing peristaltic transport with heat and mass transmission through a rectangular passage, Ellahi *et al.,* [7] used two- and three-dimensional graphs to analyse the effects of different parameters. They concluded that wall shear stress is reduced by shear thinning. Akram *et al.,* [8] discovered how the peristaltic transport of Bingham fluid in a gradient magnetic field through a conduit with various wave patterns was affected by the combined effects of heat and mass transmission. In peristaltic transport of Maxwell's fluid with crawling transport, Saleem and Haider [9] acknowledged the impacts of mass transportation and heat in addition to the Soret effect. Bhatti *et al.,*'s [10] extensive analysis of the combined effects of mass and heat transfer on the peristaltic conveyance of a two-phase Sisko fluid further examined the influence of relevant parameters on profile variations. When Hosham and Hafez [11] noticed the bifurcation phenomenon using peristaltic non-Newtonian model conveyance, where heat and mass are transferred via an axisymmetric channel, they discovered that the peristaltic features and the fluid bolus trapping were well-defined with varying single control bifurcation parameters. The effects of mass transfer, heat, and the non-Newtonian model fluid on peristaltic transport have all been studied in significant detail in the literature. The term "slip velocity" describes the difference in velocity between liquids when two-phase mixtures enter a pipe vertically. Since slip at the borders is a constant in real systems and makes experimental detection challenging, the slip conditions of the Maxwellian fluid's peristaltic flow through an axisymmetric cylindrical tube were investigated by El-Shehawy *et al.,* [12]. Further analysis was conducted by Abumandour *et al.,* [13] on the peristaltic flow of a particle-fluid suspension in an asymmetric 2-dimensional channel under slip circumstances. Further analysis was conducted by Abumandour *et al.,* [13] on the peristaltic flow of a particle-fluid suspension in an asymmetric 2-dimensional channel under slip circumstances. who found that slip parameters have a major impact on velocity control. Vajravelu *et al.,* [14] analysed how temperature slip, velocity slip, and concentration leap affected the Carreau fluid's peristaltic transport in a non-uniform route with mass and heat transfer. They observed that as the velocity slip parameter increases, so does the trapping bolus size. As Kamel *et al.,* [15] found when they examined the

peristaltic pumping brought on by a traveling sinusoidal current in the walls of a two-dimensional channel filled with a viscous incompressible fluid combined with rigid particles in the form of spheres and considered slide on the walls, the phenomenon of reflux is influenced by slip conditions. Vaidya *et al.,* [16] examined how slip affected the non-Newtonian Jeffrey fluid's peristaltic flow via a slopy tube. The impact of slip boundary conditions on temperature and axial velocity profiles was shown by Ibrahim and Abou-Zeid [17] in their analysis of how velocity slip affects the magneto nano peristaltic motion of a Prandtl fluid in an uneven channel while transferring mass and heat. The peristaltic pumping region and magnitude of the entrapped boluses decrease with increment on slip parameter, according to Khan *et al.,*'s [18] examination of the effects of slip on the peristaltic delivery of an incompressible non-Newtonian model with variable viscosity.

Viscosity and thermal conduction are two fluid properties that are typically taken for granted in research. However, when it comes to biofluids, these properties are crucial in regulating the fluid flow's temperature and velocity. According to recent research, they differ in response to temperature variations and other pertinent circumstances. While focusing on physiological modelling processes, researchers were enthralled by the realization that a mathematical model might alter the properties of fluids. Vaidya *et al.,*'s work [19] looked at the Rabinowitsch fluid's peristaltic process on a compliant porous tube. They found that, although only marginally increasing the trapped bolus magnitude, the variable viscosity parameter improves the temperature and velocity profiles. According to Choudhari *et al.,*'s [20] analysis of the peristaltic transport of Jeffrey fluid in a non-uniform channel, varying viscosity and thermal conductivity greatly enhance temperature and velocity profiles. Moreover, fluctuating viscosity is particularly important in regulating the velocity at the middle portion, based on research conducted by Balachandra *et al.,* [21] on how different liquid properties affect the Bingham fluid's peristaltic process when it passes through a porous channel. Vaidya *et al.,* [22] investigated the peristaltic conveyance of the Carreau-Yasuda fluid model with partial slip-on and magnetic effect. Higher magnetic effect, increased fluid resistance, and decreased fluid velocity are all brought on by larger viscosity parameters. In their investigation of the effects of thermal radiation on the peristaltic transport of the Casson fluid through a porous channel with variable liquid properties, Basha *et al.,* [23] found that thermal conductivity and variable viscosity increase the temperature profile while decreasing the velocity profile. Later Akbar *et al.,* [24] analysed the peristaltic flow of thermal engineering nano models with variable liquid properties within a flexible tube, observed that velocity field increases with increase in viscosity parameter near the walls and decreases to the centre of the tube.

To clarify how fluid particles and the flow medium interact on a beat, Das and Chakraborty [25] devised the concept of employing electricity for peristaltic flow. These gadgets are commonly used in the biological and medical fields. They also call their lab-on-a-chip systems microfluidic systems. Later, with the combined action of the magnetic field and electrokinetic force, Ranjit and Shit [26] studied the entropy origination in a slim fluidic field created from a uniform peristaltic current. They discovered that the centre has the lowest entropy generations, while the areas closest to the walls have the most. Additionally, Noreen *et al.,* [27] investigated the heat transfer analysis of electroosmotic transport via a Darcy-porous medium in a peristaltic mechanism. They observed that the axial velocity surged near the wall and decreased in the centre as the Darcy number increased. The electroosmotically induced peristaltic Casson fluid flow across a cylindrical tube was then studied by Saleem *et al.,* [28], who demonstrated that the flow could be completely regulated by the electric field. In a recent study, Tanveer *et al.,* [29] investigated how electroosmosis affected the non-Newtonian model's peristalsis in a microchannel with MHD. The long wavelength and low Reynolds number assumptions were applied. The parameters electroosmotic velocity, variable thermal conductivity, and variable viscosity coefficient have a major influence on velocity, concentration, and

temperature profiles, according to research conducted most recently by Choudhari *et al.,* [30]. This was done by developing a model to analyse the electrokinetic transmission through peristaltic current in a microchannel. Recently Akram and Akbar [31] analysed the electroosmotic modulated peristaltic transport of propylene glycol and Titania nano particles, identified that velocity of the fluid augmented by decreasing the thickness of electrical double layer and raising the strength of the electric field, in the forwarding direction. Further Akbar and Muhammad [32] analysed the key features of cilia propulsion for a non-Newtonian couple stress fluid with electroosmosis and heat transfer, noticed that electroosmotic velocity rises the pressure rise for symmetric and asymmetric conduits also size of formed boluses increases with rising values of electroosmotic velocity. Most recently Akbar *et al.,* [33] investigated the peristaltic propulsion of non-Newtonian micropolar fluid, with the electroosmosis and heat transfer using nanoparticles, disclosed that electroosmotic velocity directly proportional to velocity and pressure gradient for nanoparticles.

Powell and Eyring developed a fluid model known as the Eyring-Powell model in 1944. The model exhibits a non-Newtonian nature with its numerous applications in science and technology. In a recent study, Akbar and Nadeem [34] examined the effects of Eyring-Powell fluid on peristaltic flow in an endoscope by analysing the features of heat and mass transmission on peristalsis. The peristaltic conveyance of the fluid with an artificial magnetic field by Noreen and Qasim [35] reveals that Eyring-Powell fluid material constants A and B behave differently in velocity and temperature profiles. Abbasi *et al.,* [36] simulated the peristaltic transport of Eyring Powell fluid in a curved channel. The axial velocity, temperature distribution, and concentration were found to be significantly impacted by the Eyring Powell fluid characteristics, as was the case in Hina's [37] study regarding the effects of slip and magnetohydrodynamics on the peristaltic transport of the Eyring Powell model with heat transmission. Eyring Powell material constants tend to lower the fluid's temperature and velocity, according to Bhattacharyya *et al.,*'s [38] investigation into the peristaltic conveyance of the Eyring-Powell model along uniform and non-uniform passages. Additionally, they noticed that a non-uniform passage's temperature and velocity are higher than those of a uniform channel. Recently Rehman *et al.,* [39] used artificial intelligence to analyse the peristaltic transport of thermal flow of Eyring Powell fluid with identical free stream and heated stretched porous boundaries, shown that skin friction coefficient shows higher values for enhanced Eyring Powell fluid material constants. Most recently Rehman and Shatanawi [40] developed a machine learning remedy to investigate the mass transfer effects of peristaltic transport of Eyring-Powell fluid, observed that Eyring Powell fluid parameters have a significant effect on controlling the mass transfer.

The literature motivates the authors to integrate the effects of electroosmosis, slip boundary conditions, and changeable liquid properties on the peristaltic transport of non-Newtonian fluid, due to their relevance on blood flow analysis and peristaltic pumping mechanisms, which has received little attention to date. The present model examines the peristaltic conveyance of the Eyring-Powell model while accounting for slip and the variable liquid properties under the influence of an electric field. The long wavelength and low Reynolds number assumptions are taken into consideration, and the continuity, momentum, and energy equations are assumed to be the governing equations Once the variables have been nondimensionalized, the nonlinear equations are solved via the perturbation method. MATLAB R2023a programming is used to express the effects of relevant parameters on streamlines, temperature, and velocity. The results can be applied to study the effects of different parameters on different engineering and biological domains.

2. Methodology

2.1 Formulation of the Problem

The two-dimensional peristaltic transport of the Eyring-Powell model as shown in Figure 1 is studied in a non-uniform passage with slip boundary conditions and changing fluid characteristics under the influence of an electric field. The mass characterisation coefficient, wall damping coefficient, and wall tension coefficients were among the wall attributes considered during the modelling process.

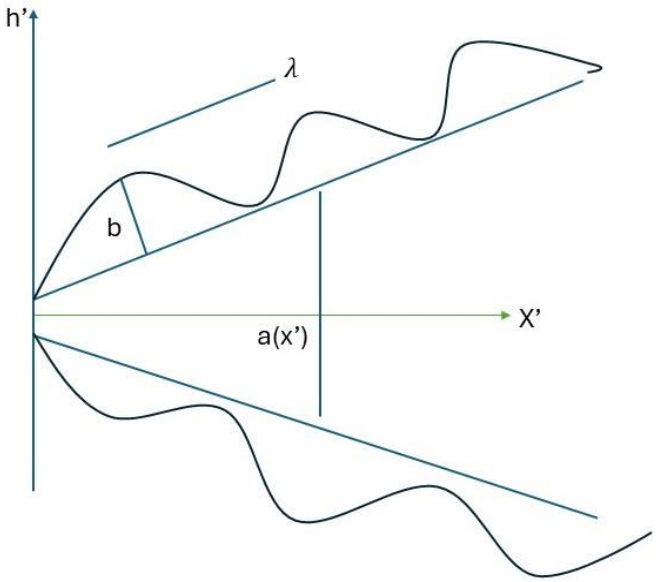

Fig. 1. Geometry of the physical model

The channel's geometry can be expressed as given by

$$h' = a(x') + \mathrm{b\ si\ n}\left[\frac{2\pi}{\lambda}(x' - ct')\right] \tag{1}$$

where $\mathrm{a(x')}$ is the nonuniform radius, *b* is the wave amplitude, c' is the wave speed, and h' is the nonuniform wave, t' is the time.

Now the governing equations, we consider the equation of continuity, equations of momentum, and equation of energy:

$$\frac{\partial u'}{\partial x'} + \frac{\partial u'}{\partial y'} = 0 \tag{2}$$

$$\rho\left(\frac{\partial u'}{\partial t'} + u'\frac{\partial u'}{\partial x'} + v'\frac{\partial u'}{\partial y'}\right) = -\frac{\partial p'}{\partial x'} + \frac{\partial \tau_{x'x'}}{\partial x'} + \frac{\partial \tau_{x'y'}}{\partial y'} + \rho_e E_0 \tag{3}$$

$$\rho\left(\frac{\partial v'}{\partial t'} + u'\frac{\partial v'}{\partial x'} + v'\frac{\partial v'}{\partial y'}\right) = -\frac{\partial p'}{\partial x'} + \frac{\partial \tau_{y'x'}}{\partial x'} + \frac{\partial \tau_{y'y'}}{\partial y'} \tag{4}$$

$$\rho c_p\left(\frac{\partial v'}{\partial t'} + u'\frac{\partial v'}{\partial x'} + v'\frac{\partial v'}{\partial y'}\right) = \mathrm{k}\left(\frac{\partial^2 T'}{\partial x'^2} + \frac{\partial^2 T'}{\partial y'^2}\right) + \left[\frac{\partial u'}{\partial x'}\left(\tau_{x'x'}, \tau_{y'y'}\right) + \left(\frac{\partial u'}{\partial x'} + \frac{\partial u'}{\partial y'}\right)\tau_{x'y'}\right] \tag{5}$$

where ρ is the fluid density, ρ_e is the electrical charge density, p' is the pressure, and E_0 is the axial electric field, and u', v' are the components of velocity in the x' and y' directions. Where c_p is the specific heat at constant pressure and T' is the temperature. The additional stress components are $\tau_{x'x'}, \tau_{x'y'}, \tau_{y'x'},$ and $\tau_{y'y'}$.

We now consider the nondimensionalization parameters.

$$h = \frac{h'}{a},\ t = \frac{ct'}{\lambda},\ x = \frac{x'}{\lambda},\ y = \frac{y'}{a},\ u = \frac{u'}{c},\ v = \frac{v'}{\alpha c},\ \alpha = \frac{a}{\lambda},\ p = \frac{p'a^2}{c\mu},\ k = \frac{a}{\lambda_D},\ \psi = \frac{\psi'}{ca},\ P_e = \frac{c\lambda}{d},$$

$$\theta = \frac{T'-T_0}{T_1-T_0},\ U_{hs} = \frac{-E_x \epsilon \epsilon_0}{c\mu},\ B_r = E_c.P_r,\ R_e = \frac{\rho ca}{\mu},\ P_r = \frac{\mu c_p}{k},\ \tau_{ij} = \frac{a}{\mu c}\tau_{i'j'},\ E_c = \frac{c^2}{c_p(T_1-T_0)}, \quad (6)$$

where U_{hs} is the electroosmotic velocity, k is the electroosmotic parameter, p is the non-dimensional pressure, ϕ is the nondimensional wave amplitude, and x, y are the non-dimensional axial and transverse coordinates. "a" is the semi-breadth of the channel, "λ_D " is the Debye length, "h" is the transverse non-dimensional wall vibration, and "ψ" is the non-dimensional stream function. Non-dimensional shear stress (τ), Brinkman number (Br), Prandtl number (Pr), Reynolds number (Re), Eckert number (E_c), where ϵ_0 is the permittivity in free space, T0 is the absolute temperature, and ϵ is the permittivity of the medium.

Following the non-dimensionalization of the variables, the governing equations (2) through (5) take on the assumptions of a long wavelength and a low Reynolds number also analysing the previous works of Akbar and Nadeem [41] and Gudekote *et al.,* [42]

$$\frac{\partial p}{\partial x} = \frac{\partial \tau_{xy}}{\partial y} + k^2\, U_{hs}\, \phi \quad (7)$$

$$\frac{\partial p}{\partial y} = 0 \quad (8)$$

$$\frac{\partial}{\partial y}\left[K(\theta)\frac{\partial \theta}{\partial y}\right] + B_r\, \tau_{xy}\frac{\partial^2 \psi}{\partial y^2} = 0 \quad (9)$$

$$\frac{\partial^2 \sigma}{\partial y^2} + S_c S_r \frac{\partial^2 \theta}{\partial y^2} = 0. \quad (10)$$

Since the flow is non-Newtonian, Eyring-Powell fluid model the extra stress component [41],

$$\tau_{xy} = (\mu(y) + B)\frac{\partial^2 \psi}{\partial y^2} - \frac{A}{3}\left(\frac{\partial^2 \psi}{\partial y^2}\right)^3, \quad (11)$$

where, $\phi = \frac{coshky}{coshkh}$, ϕ is the electric potential.

The Eyring-Powell model's material constants are A and B, the electroosmotic parameter is k, the Brinkman number is Br, the Schmidth number is Sc, and the Soret number is Sr.

According to the non-dimensional boundary conditions,

$$\psi = F,\ at\ y = 0 \qquad \frac{\partial \psi}{\partial y} + \beta_1 \tau_{xy} = -1 \text{ at } y = h, \quad (12)$$

$$h = 1 + mx + \varepsilon \sin[2\pi(x - t)] \quad (13)$$

$$\frac{\partial \theta}{\partial y} = 0, \ at \ y = 0, \tag{14}$$

$$\theta + \beta_2 \frac{\partial \theta}{\partial y} = 1, at \ \ \text{y = h}, \tag{15}$$

$$\frac{\partial \sigma}{\partial y} = 0, \ at \ \ y = 0, \tag{16}$$

$$\sigma + \beta_3 \frac{\partial \sigma}{\partial y} = 1, at \ \ \text{y = h} \tag{17}$$

The varying viscosity $\mu(y)$ and thermal conductivity K(θ) given as

$$\mu(y) = 1 - \alpha_1 y, \quad \alpha_1 \ll 1. \tag{18}$$

$$\text{K}(\theta) = 1 + \alpha_2 \theta, \qquad \alpha_2 \ll 1.$$

On considering the wall properties, expression for pressure becomes,

$$\frac{\partial p}{\partial x} = \frac{8\pi^3 \varepsilon(-(E_1 - E_2))cos2\pi(x-t) + (E_3 sin(2\pi(x-t))}{2\pi} \tag{19}$$

where E_1 is the wall tension coefficient, E_2 is the mass characterization coefficient, E_3 is the wall damping coefficient.

2.2 Solution Methodology

The nature of Eq. (7) and Eq. (9) is nonlinear, computing the analytical solutions is tedious. We apply perturbation technique as a semi analytical method to solve the system of equations. Comparing Eq. (7) and Eq. (19), we get,

$$\frac{\partial p}{\partial x} = (1 - \alpha_1 y + \text{B}) \frac{\partial^3 \psi}{\partial y^3} - \frac{A}{3}\left(\frac{\partial^2 \psi}{\partial y^2}\right)^3 + k^2 \ \text{U}_{\text{hs}} \ \phi. \tag{20}$$

$$\frac{\partial p}{\partial x} = \frac{8\pi^3 \varepsilon((-(E_1 - E_2))cos2\pi(x-t) + (E_3 sin(2\pi(x-t)))}{2\pi} \tag{21}$$

$$\frac{\partial}{\partial y}[(1 + \ \alpha_2 \theta) \ \frac{\partial \theta}{\partial y}] + B_r[(\mu(y) + B) \frac{\partial^2 \psi}{\partial y^2} - \frac{A}{3}\left(\frac{\partial^2 \psi}{\partial y^2}\right)^3] \frac{\partial^2 \psi}{\partial y^2} = 0 \tag{22}$$

2.2.1 Perturbation method

We assume the series solution expression as,

$$\psi = \sum_{n=0}^{\infty} A^n \psi_n \tag{23}$$

$$\theta = \sum_{n=0}^{\infty} A^n \theta_n \tag{24}$$

Assuming the perturbation parameter A is so small by neglecting the higher-degree terms,

Zeroth order system

$$(1-\alpha_1 y + B)\frac{\partial^2 \psi_0}{\partial y^2} + k^2 U_{hs}\frac{sinhky}{coshkh} = Py \quad (25)$$

$$\frac{\partial \theta_0}{\partial y}+\alpha_2\theta_0\frac{\partial \theta_0}{\partial y}+\int (B_r(1-\alpha_1 y + B)\frac{\partial^2 \psi_0}{\partial y^2})dy = 0 \quad (26)$$

where, $P = \frac{\partial p}{\partial x}$, Corresponding boundary conditions are,

ψ_0 = F, at y = 0, and $\frac{\partial \psi_0}{\partial y} + \beta_1\tau_{xy} = -1$, at y = h

$\frac{\partial \theta_0}{\partial y} = 0\ at\ y = 0$, and $\theta_0 + \beta_2\frac{\partial \theta_0}{\partial y} =$ -1 at y = h.

First order system

$$(1-\alpha_1 y + B)\frac{\partial^2 \psi_1}{\partial y^2} = \frac{1}{3}\left(\frac{\partial^2 \psi_0}{\partial y^2}\right)^3 \quad (27)$$

$$\frac{\partial \theta_1}{\partial y}+\alpha_2\theta_0\frac{\partial \theta_1}{\partial y}+\alpha_2\theta_1\frac{\partial \theta_0}{\partial y}+\int (B_r\{2(1-\alpha_1 y + B)\frac{\partial^2 \psi_0}{\partial y^2}\frac{\partial^2 \psi_1}{\partial y^2} - \frac{1}{3}\left(\frac{\partial^2 \psi_0}{\partial y^2}\right)^4)dy = 0 \quad (28)$$

Corresponding boundary conditions, given by

ψ_1 = 0, at y = 0, and $\frac{\partial \psi_1}{\partial y} + \beta_1\tau_{xy} = 0$, at y = h

$\frac{\partial \theta_1}{\partial y}$ = 0 at y = 0, and $\theta_1 + \beta_2\frac{\partial \theta_1}{\partial y} = 0$ at y = h.

Due to the nonlinearity of Eq. (25), Eq. (26), Eq. (27) and Eq. (28) we use the double perturbation method.

$$\psi_0 = \psi_{00} + \alpha_1\psi_{01} \quad (29)$$

$$\psi_1 = \psi_{10} + \alpha_1\psi_{11} \quad (30)$$

$$\theta_0 = \theta_{00} + \alpha_2\theta_{01} \quad (31)$$

$$\theta_1 = \theta_{10} + \alpha_2\theta_{11} \quad (32)$$

The zeroth order streamline equations become,

$$\frac{\partial^2 \psi_{00}}{\partial y^2} = \frac{1}{1+B}\{Py - kU_{hs}\frac{sinhky}{coshkh}\} \quad (33)$$

$\frac{\partial^2\psi_{01}}{\partial y^2}=\frac{y}{1+B}\frac{\partial^2\psi_{00}}{\partial y^2}$ (34)

The associated boundary conditions are as follows:

$\psi_{00}=F,\ \psi_{01}=0$ at $y=0$;

$\frac{\partial\psi_{00}}{\partial y}+\beta_1(1+B)\frac{\partial^2\psi_{00}}{\partial y^2}$=-1, $\frac{\partial\psi_{01}}{\partial y}+\beta_1(1+B)\frac{\partial^2\psi_{01}}{\partial y^2}-\beta_1 y\frac{\partial^2\psi_{00}}{\partial y^2}$=0 at *y* = h: (35)

First order streamline equations become,

$\frac{\partial^2\psi_{10}}{\partial y^2}=\frac{1}{3(1+B)}(\frac{\partial^2\psi_{00}}{\partial y^2})^3$; (36)

$\frac{\partial^2\psi_{11}}{\partial y^2}=\frac{y}{1+B}\frac{\partial^2\psi_{10}}{\partial y^2}+\frac{1}{3(1+B)}(\frac{\partial^2\psi_{00}}{\partial y^2})^2\frac{\partial^2\psi_{01}}{\partial y^2}$. (37)

The corresponding boundary conditions that apply are,

$\psi_{10}=0,\ \psi_{11}=0$ at $y=0$; (38)

$\frac{\partial\psi_{00}}{\partial y}+\beta_1(1+B)\frac{\partial^2\psi_{10}}{\partial y^2}-\frac{\beta_1}{3}(\frac{\partial^2\psi_{00}}{\partial y^2})^3$ = 0;

$\frac{\partial\psi_{11}}{\partial y}+\beta_1(1+B)\frac{\partial^2\psi_{11}}{\partial y^2}-\beta_1 y\frac{\partial^2\psi_{10}}{\partial y^2}-\beta_1\left(\frac{\partial^2\psi_{00}}{\partial y^2}\right)^2\frac{\partial^2\psi_{01}}{\partial y^2}$.=0, at *y* = h (39)

The zeroth order temperature equations are,

$\frac{\partial\theta_{00}}{\partial y}+\int B_r\{(1-\alpha_1 y+B)(\frac{\partial^2\psi_0}{\partial y^2})^2\}$dy = 0 (40)

$\frac{\partial\theta_{01}}{\partial y}+\theta_{00}\frac{\partial\theta_{00}}{\partial y}$ = 0 (41)

With corresponding boundary conditions

$\frac{\partial\theta_{00}}{\partial y}=0$, and $\frac{\partial\theta_{01}}{\partial y}$ = 0, at y = 0 (42)

$\theta_{00}+\beta_2\frac{\partial\theta_{00}}{\partial y}=1, and\ \theta_{01}+\beta_2\frac{\partial\theta_{01}}{\partial y}$=0; at y = h. (43)

First order temperature equations,

$\frac{\partial\theta_{10}}{\partial y}+\int B_r\{2(1-\alpha_1 y+B)((\frac{\partial^2\psi_0}{\partial y^2})((\frac{\partial^2\psi_1}{\partial y^2})-\frac{1}{3}\left(\frac{\partial^2\psi_{00}}{\partial y^2}\right)^4\}dy=0$; (44)

$\frac{\partial\theta_{11}}{\partial y}+\theta_{00}\frac{\partial\theta_{10}}{\partial y}+\theta_{10}\frac{\partial\theta_{00}}{\partial y}$ = 0 (45)

With boundary conditions

$\frac{\partial \theta_{10}}{\partial y} = 0$, and $\frac{\partial \theta_{11}}{\partial y}$=0, at y = 0; (46)

$\theta_{10} + \beta_2 \frac{\partial \theta_{10}}{\partial y} = 0, and\ \theta_{11} + \beta_2 \frac{\partial \theta_{11}}{\partial y}$=0; at y = h. (47)

After solving the equations, we get the streamline and temperature functions in the form,

$$\psi = \psi_{00} + \alpha_1 \psi_{01} + A\psi_{00}\psi_{10} + A\alpha_1 \psi_{11} \quad (48)$$

$$\theta = \theta_{00} + \alpha_2 \theta_{01} + A\theta_{10} + A\alpha_2 \theta_{11} \quad (49)$$

Using u=$\frac{\partial \psi}{\partial y}$, we get the expression for axial velocity, and solving Eq. (10) analytically to get the expression for concentration σ.

The solutions obtained using double perturbation method can be listed as

$$\psi_{00} = \frac{1}{(1+B)}\left[\frac{py^3}{6} - \frac{kU_{hs}.sinhky}{coshkh.k^2}\right] + c_1 y + F$$

$$\psi_{01} = \frac{1}{(1+B)^2}\left[\frac{py^4}{12} - \frac{yU_{hs}.sinhky}{coshkh.k} + \frac{2.U_{hs}.coshky}{coshkh.k^2}\right] + c_2 y + c_3$$

$$\psi_{10} = \frac{1}{3(1+B)^4}\{\frac{p^3y^5}{20} - \frac{k^2{U_{hs}}^3}{4cosh^3kh}\left(\frac{sinh3ky}{9k} - \frac{3sinhky}{k}\right) - \frac{3p^2U_{hs}}{coshkh}\left(\frac{y^2sinhky}{k} - \frac{2ycoshky}{k^2} + \frac{2sinhky}{k^3}\right) + \frac{3pk^2{U_{hs}}^2}{cosh^2kh}(\frac{ycosh2ky}{4k^2} - \frac{sinh2ky}{8k^3} - \frac{y^2}{2})\} + c_4 y.$$

$$\psi_{11} = \frac{4}{3(1+B)^5}\{\frac{p^3y^6}{30} - \frac{k^2{U_{hs}}^3}{4cosh^3kh}\left(\frac{ysinh3ky}{9k} - \frac{2cosh3ky}{27k^2} - \frac{3sinhky}{k}\right) - \frac{3p^2U_{hs}}{coshkh}\left(\frac{y^2sinhky}{k} - \frac{4ycoshky}{k^2} + \frac{6sinhky}{k^3}\right) + \frac{3pk^2{U_{hs}}^2}{cosh^2kh}(\frac{ycosh2ky}{4k^2} - \frac{sinh2ky}{4k^3} - \frac{y^2}{2})\} + c_5 y + c_6$$

$$c_1 = \frac{-1}{1+B}\left[\frac{ph^2}{2} - U_{hs}\right] - \beta_1\left[ph - kU_{hs}\frac{sinhkh}{coshkh}\right] - 1$$

$$c_2 = \frac{1}{(1+B)^2}[\frac{ph^3}{3}U_{hs}(h+\frac{sinhkh}{coshkh})].$$

$$c_3 = \frac{-2.U_{hs}}{(1+B)^2 coshkh.k^2}$$

$$c_4 = \frac{1}{3(1+B)^4}[\frac{p^3h^4}{4} - \frac{k^2{U_{hs}}^3}{12cosh^3kh} - \frac{k^2{U_{hs}}^3}{4cosh^2kh} - 3p^2U_{hs}.h^2 + \frac{3phk^2\,{U_{hs}}^2 sinh2kh}{2k.cosh^2kh} - 3p\frac{k^2\,{U_{hs}}^2h^2}{4cosh^2kh}.$$

$$c_5 = \frac{4}{3(1+B)^5}[\frac{p^3h^5}{5} - \frac{k^3\,{U_{hs}}^3}{4cosh^3kh}\left(\frac{hcosh3kh}{3k} - \frac{sinh3kh}{9k^2} - \frac{3coshkh}{k}\right) - \frac{3p^2U_{hs}}{coshkh.}\left(coshkh.h^2 - \frac{2hsinhkh}{k} + \frac{2coshkh}{k^2}\right) + \frac{3pk\,{U_{hs}}^2}{2}(hsinh2kh - \frac{cosh2kh}{2k} - 2kh)$$

$c_6 = \frac{-4{U_{hs}}^3}{81(1+B)^5 cosh^3 kh}$.

3. Results and Discussions

Effects of various relevant parameters on velocity, temperature, concentration, and streamline profiles are analysed through graphical representations using MATLAB R2022a programming. The parameters that were selected are the material constants (A and B) of the Eyring-Powell model, the non-uniform parameter (m), the electroosmotic velocity (U_{hs}), the electroosmotic parameter (k), the velocity slip parameter (β_1), the thermal slip parameter (β_2), variable viscosity parameter (α_1) variable thermal conductivity parameter (α_2), amplitude ratio (ϵ), concentration slip parameter (β_3), and wall properties (E_1 to E_3).

3.1 Velocity Profiles

Variation of velocity profiles along with the pertinent parameters are exhibited through Figure 2(a) to Figure 2(i). Figure 2(a) depicts the effects of non-uniform parameter *(m)* on the velocity profiles, which narrates an increment in parameter *(m)* reflects in enhanced velocity. Figure 2(b) has sketched to identify the electroosmotic velocity *(U_{hs})* has a significant effect on velocity profiles, increased electroosmotic velocity results enhanced velocity of fluid. Figure 2(c) is to draw the effects of electroosmotic parameter*(k)* on the velocity profiles. From the figure it has been noticed that the increased value of *k* enhances the velocity profiles. Figure 2(d) and Figure 2(e) are drawn to analyse the effect of Eyring-Powell fluid parameters A and B on velocity profiles. It has been noticed that an increased value of A results that enhanced velocity profiles, while enhanced B value declines the velocity profiles. The effect of velocity slip parameter (β_1) as increased which results in enhanced the velocity profiles (see Figure 2(f)). Figure 2(g) shows that increased value of variable viscosity parameter (α_1) enhances the velocity profiles. The effect of amplitude ratio (ϵ) on velocity profile, indicates that increased amplitude ratio results in enhanced velocity (see Figure 2(h)). Figure 2(i) releases the effect of wall properties on velocity profiles shows that increased wall tension coefficient (E_1) gives higher velocity, identifies increased mass characterisation coefficient (E_2) results enhanced velocity, also remarks increased wall damping coefficient (E_3) declines the velocity.

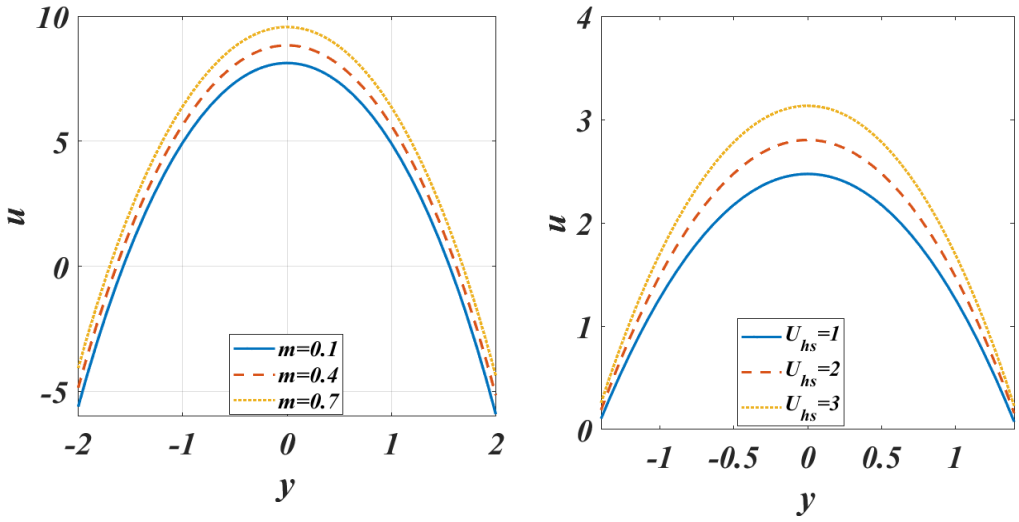

(a) (b)

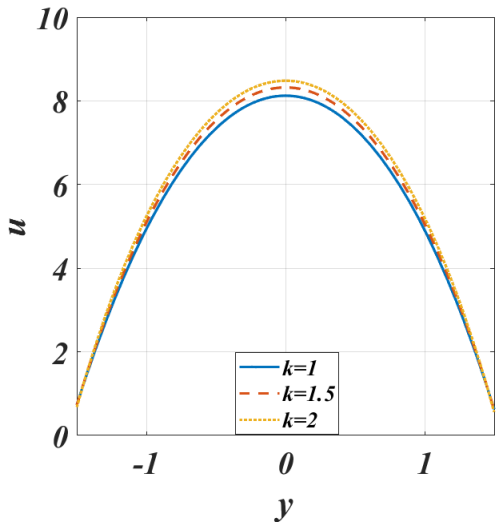
u
y
k=1
k=1.5
k=2

(c)

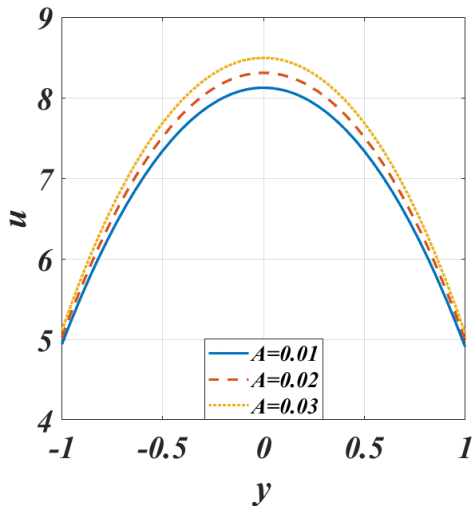
u
y
A=0.01
A=0.02
A=0.03

(d)

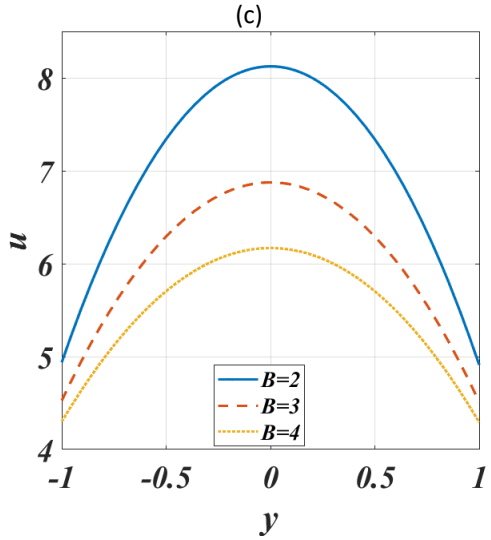
u
y
B=2
B=3
B=4

(e)

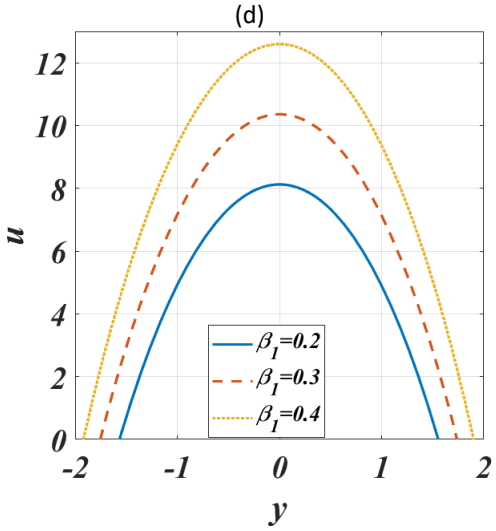
u
y
β1=0.2
β1=0.3
β1=0.4

(f)

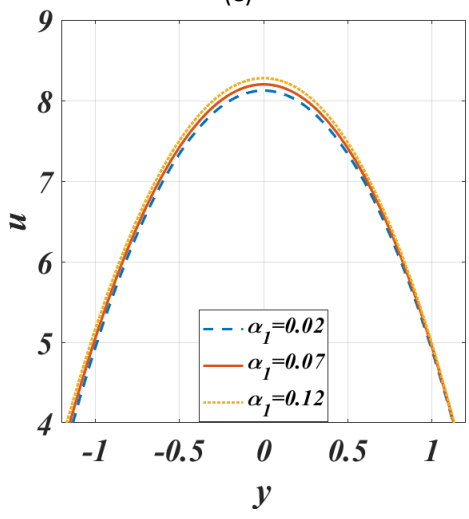
u
y
α1=0.02
α1=0.07
α1=0.12

(g)

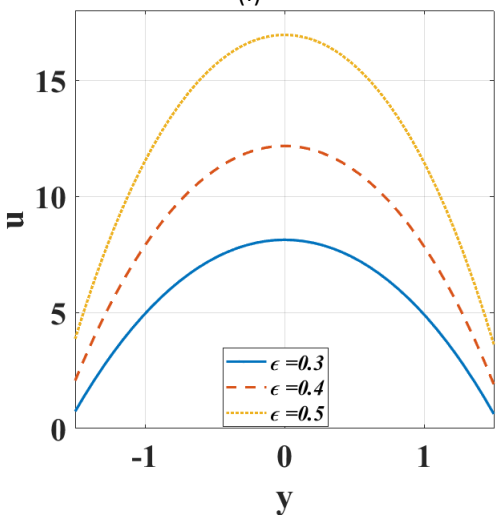
u
y
ϵ =0.3
ϵ =0.4
ϵ =0.5

(h)

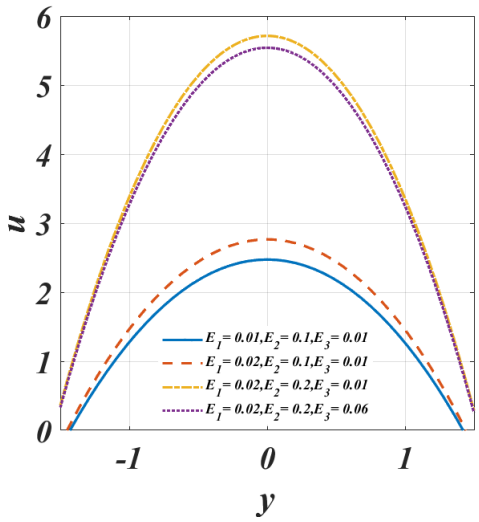

(i)

Fig. 2. Impact of different parameters on velocity profiles, (a) m, (b) U_{hs}, (c) k, (d) α_2, (e) B, (f) β_1, (g) α_1, (h) ε, (i) E_1, E_2, and E_3

3.2 Temperature Profiles

Figure 3(a) to Figure 3(k) are drawn the influences of the parameters, directly affecting the fluid flow, on the temperature profiles demonstrated through graphical representations. The efficacy of the non-uniform parameter (m) on temperature profiles is shown in Figure 3(a), which demonstrates that a greater non-uniform parameter indicates an improvement in the temperature profiles. The non-dimensional Brinkman number (Br) plays a significant role in temperature profiles explained through Figure 3(b), increased Brinkman number reflects improved temperature profiles. Thermal slip parameter (β2) increases the temperature profile (see Figure 3(c)). The variable thermal conductivity parameter (α_2) makes considerable change on the temperature profile is analysed through Figure 3(d), increasing variable thermal conductivity parameter diminishes the temperature profile. It is evident from Figure 3(e) that the temperature profile is governed by the electroosmotic velocity parameter (U_{hs}); an increase in electroosmotic velocity results in the development of a decreasing temperature profile. Increase in Electroosmotic parameter (k) results in enhanced temperature profile, explained through the Figure 3(f). As illustrated in Figure 3(g) and Figure 3(h), the Eyring-Powell fluid parameters (A & B) exhibit comparable behaviour in regulating the temperature profile; namely, they both reduce the temperature profiles. Figure 3(i) sketches that increased variable viscosity parameter (α_1) results in enhanced temperature profiles. Higher valued amplitude ratio(ϵ) provides higher temperature profile as analysed through Figure 3(j). Wall properties like, wall tension coefficient, mass characterisation coefficient, and wall damping coefficient plays significant role on temperature profiles is explained through Figure 3(k) increased wall tension coefficient and mass characterisation coefficient improves the temperature profiles, while increase in wall damping coefficient declines the temperature profiles.

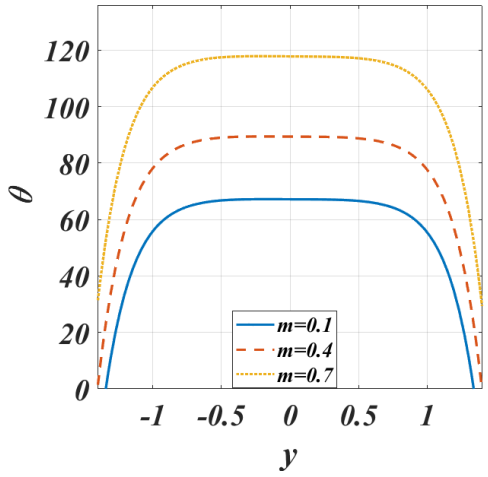
θ
y
m=0.1
m=0.4
m=0.7

(a)

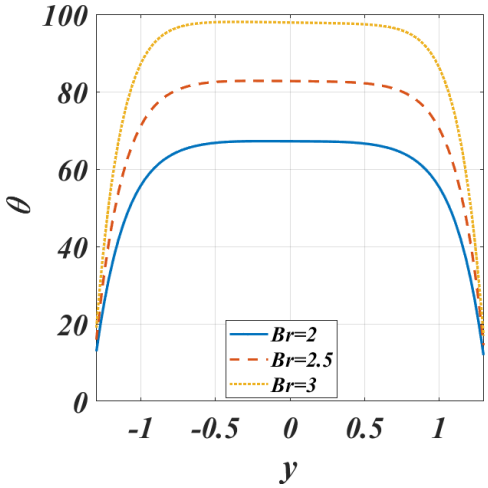
θ
y
Br=2
Br=2.5
Br=3

(b)

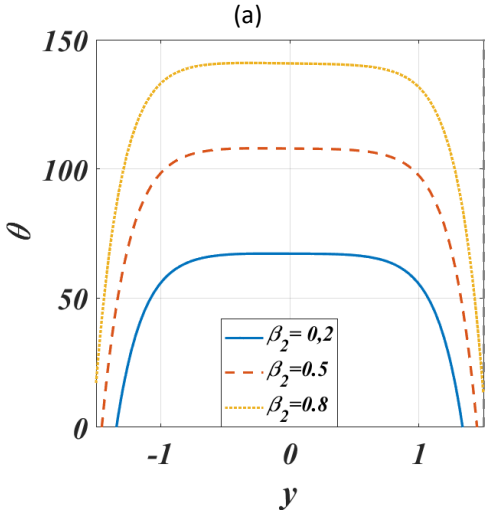
θ
y
β2= 0,2
β2=0.5
β2=0.8

(c)

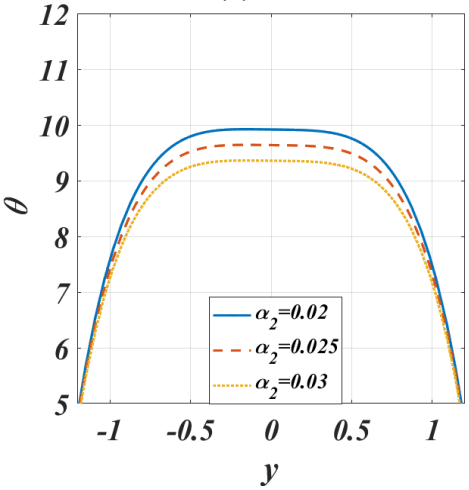
θ
y
α2=0.02
α2=0.025
α2=0.03

(d)

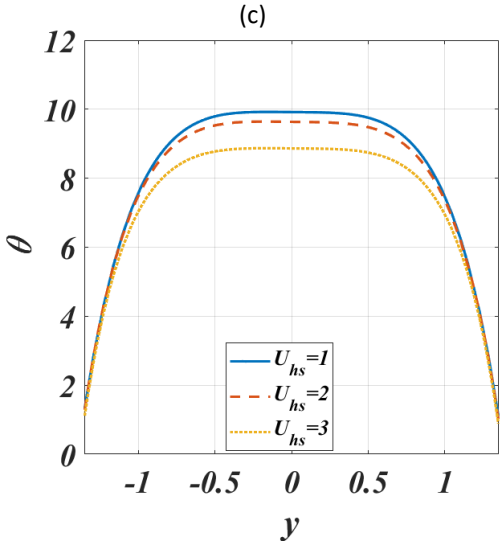
θ
y
Uhs=1
Uhs=2
Uhs=3

(e)

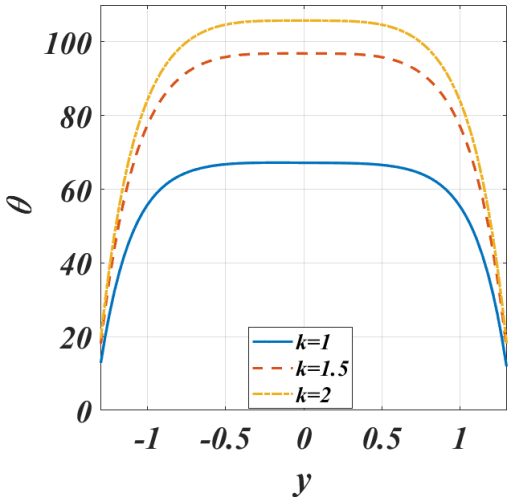
θ
y
k=1
k=1.5
k=2

(f)

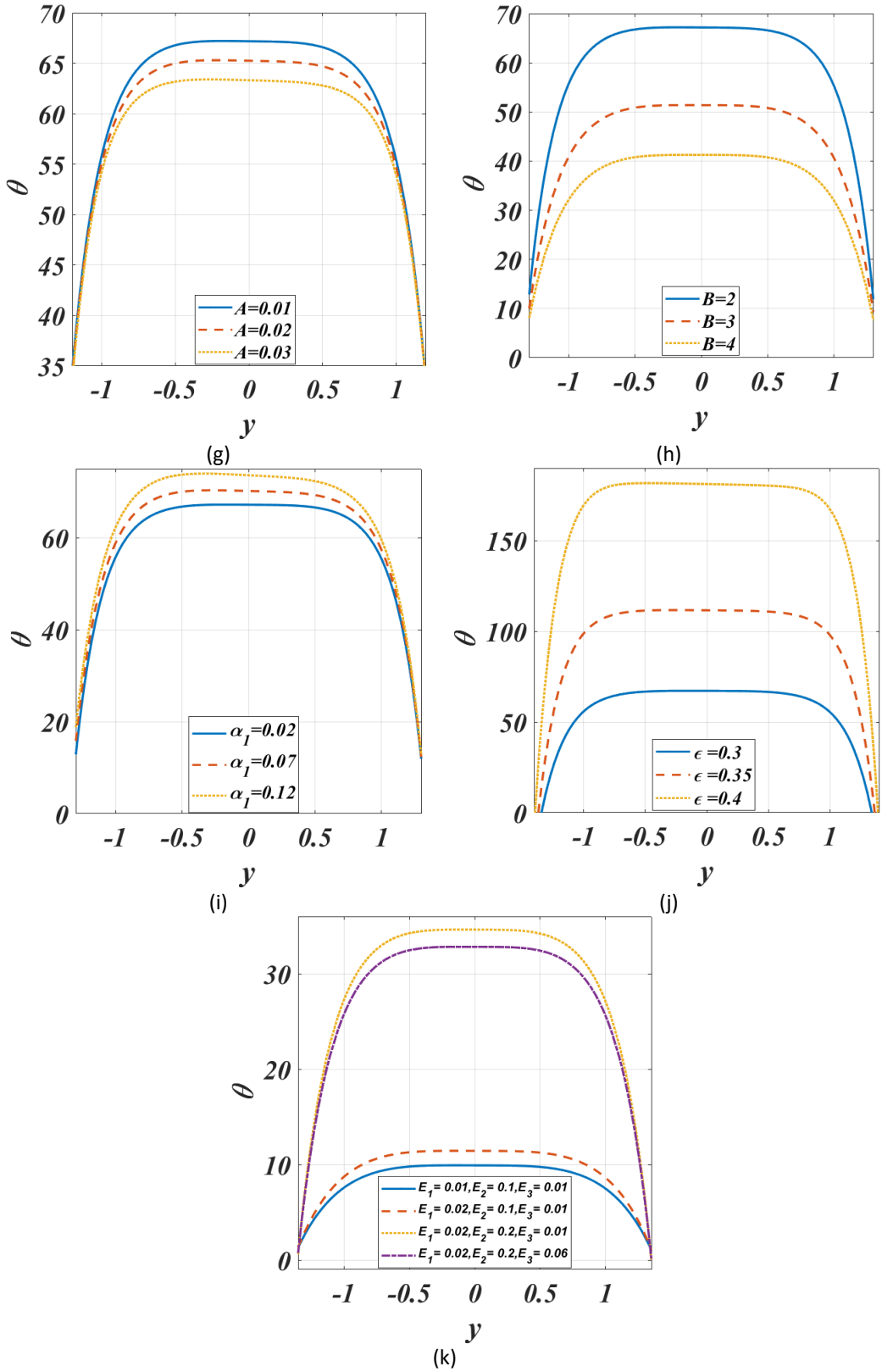

Fig. 3. Impact of different parameters on temperature profiles, (a) m, (b) Br, (c) β_2, (d) α_2, (e) U_{hs}, (f) k, (g) A, (h) B, (i) α_1, (j) ε, (k) E_1, E_2, and E_3

3.3 Concentration Profiles

Effects of different significant parameters on concentration profiles represented graphically are shown in Figure 4(a) to Figure 4(n). When the variable viscosity parameter is examined in Figure 4(a), it becomes apparent that a smaller rise in the variable viscosity parameter results in a smaller decrease in the concentration profile. While the variable thermal conductivity parameter, when increased makes a slighter enhanced concentration profile (see Figure 4(b)). The effect of the thermal slip parameter is seen in Figure 4(c): The concentration profile is diminished by an increase in the thermal slip parameter. The influence of concentration slip parameter on concentration profile is seen in Figure 4(d); a higher concentration slip parameter results in a better concentration profile. Figure 4(e) and Figure 4(f) illustrate how the Eyring-Powell fluid parameters A&B significantly affect the concentration profile, which explains the opposite behaviour seen. Increase in A declines the concentration profile, increase in B enhances the concentration profile. Figure 4(g) identifies that increase in amplitude ratio ε results in declining concentration profile. Increase in non-uniform parameter m gives diminishing concentration profile is demonstrated in Figure 4(h). Increase in electroosmotic parameter k results in diminishing concentration profile (see Figure 4(i)). The electroosmotic velocity U_{hs} also portray substantial role in controlling the concentration of the fluid flow is depicted through Figure 4(j), identifies that increase in U_{hs} value declines the concentration profile. Figure 4(k) sketched to identify that increase in Brinkmann number results in declined concentration profile. Figures 4(l) and Figure 4(m) show how different Soret and Schmidt numbers affect the concentration profile. Increase in both numbers declines the concentration profiles. The impacts of different wall characteristics (E1, E2, and E3) on the concentration profiles are shown in Figure 4(n). The concentration profile is reduced by the wall tension coefficient (E1) and mass characterisation coefficient (E2), while the concentration profile is increased by the wall damping coefficient (E3).

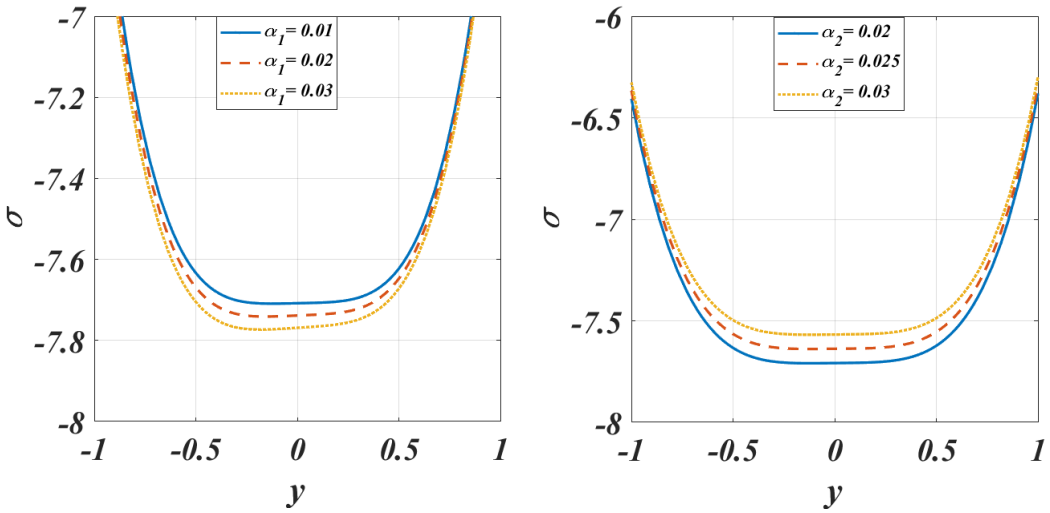

(a) (b)

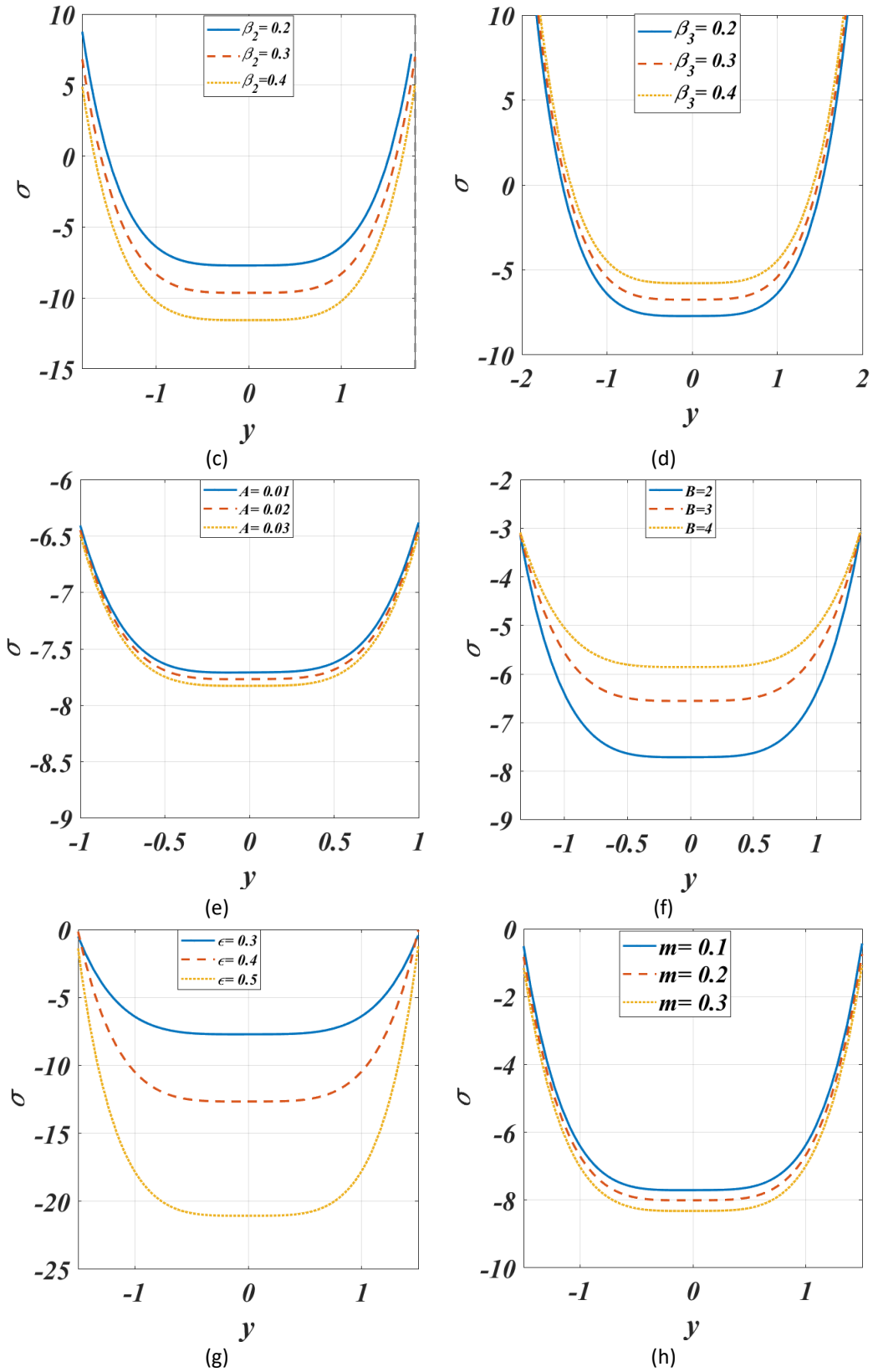
β2= 0.2
β2= 0.3
β2=0.4
σ
y
(c)
β3= 0.2
β3= 0.3
β3= 0.4
σ
y
(d)
A= 0.01
A= 0.02
A= 0.03
σ
y
(e)
B=2
B=3
B=4
σ
y
(f)
ϵ= 0.3
ϵ= 0.4
ϵ= 0.5
σ
y
(g)
m= 0.1
m= 0.2
m= 0.3
σ
y
(h)

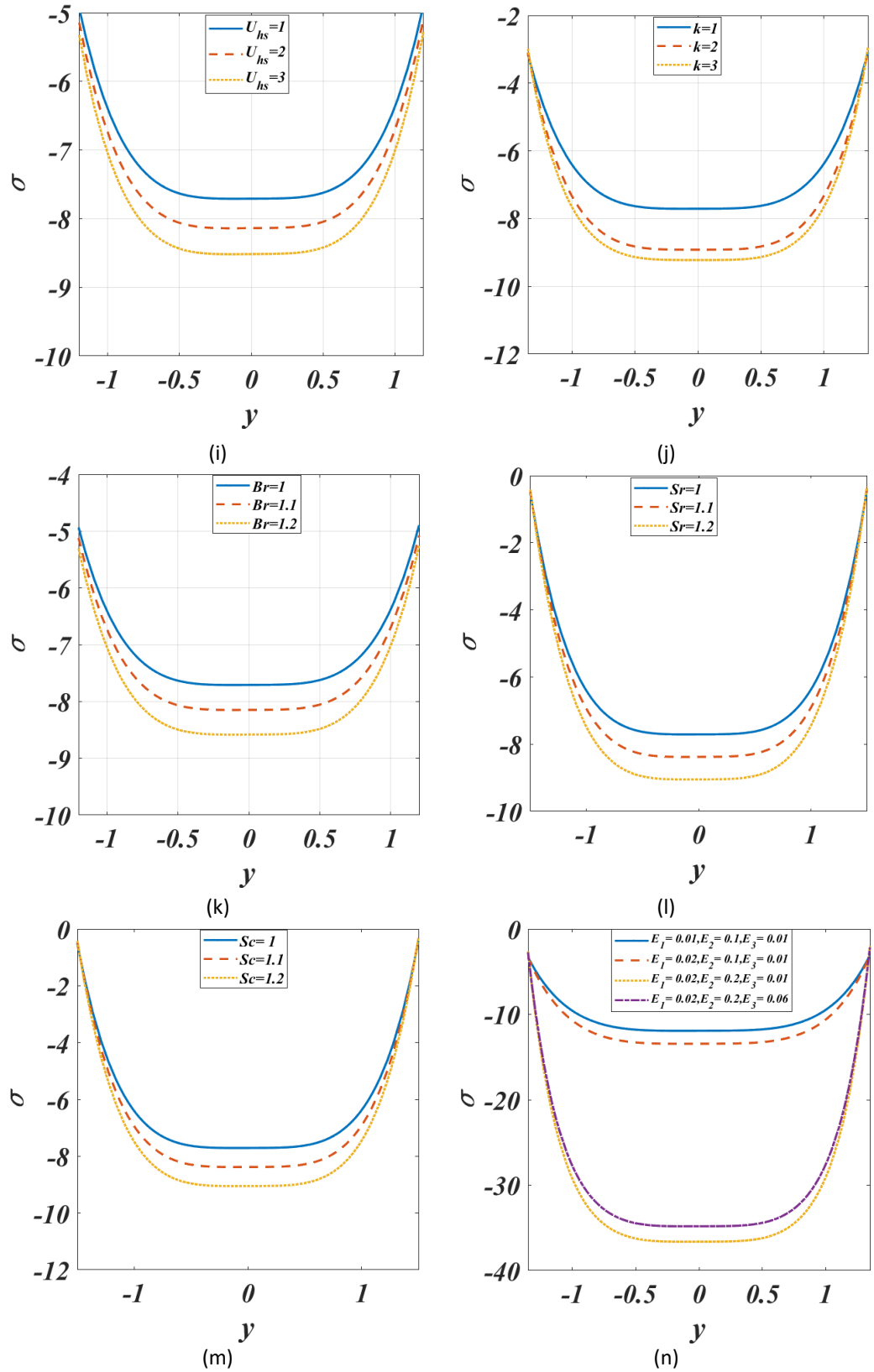

Fig. 4. Impact of different parameters on concentration profiles, (a) α_1, (b) α_2, (c) β_2, (d) β_3, (e) A, (f) B, (g) ε, (h) m, (i) U_{hs}, (j) k, (k) B_r, (l) Sr, (m) Sc, and (n) E_1, E_2, and E_3

3.4 Trapping Phenomenon

The movement of streamlines, sometimes leads to a collision, development of boluses occurs naturally. The closed streamlines and the formed boluses play a vital role, while analysing peristaltic mechanism. Through the Figure 5 to Figure 12 we try to study the role played of different parameters on deciding this trapping behaviour. Figure 5 identifies the role of Eyring-Powell model material constant A on the trapping phenomena, as the value of A increases the magnitude of the bolus increases, with same number of boluses formed. While the Eyring- Powell model material constant B decreases the number of boluses and size of the boluses (see Figure 6) In the case of the variable viscosity parameter, the number of the bolus decreases, with enhanced size as parameter of variable viscosity increases (see Figure 7). The electroosmotic velocity plays a crucial role on trapping effect can be verified through Figure 8, suggests that increased electroosmotic velocity declines the number of boluses in greater amount. Through Figure 9 increased nonuniform parameter declines the number of boluses is verified. Figure 10 suggests increased electroosmotic parameter enhances the magnitude of the boluses without affecting the number of boluses. From Figure 11, it is identified that both magnitude and number of boluses enhances with increase in amplitude ratio parameter. The quantity and size of the produced boluses are likewise increased by the velocity slip parameter (refer Figure 12).

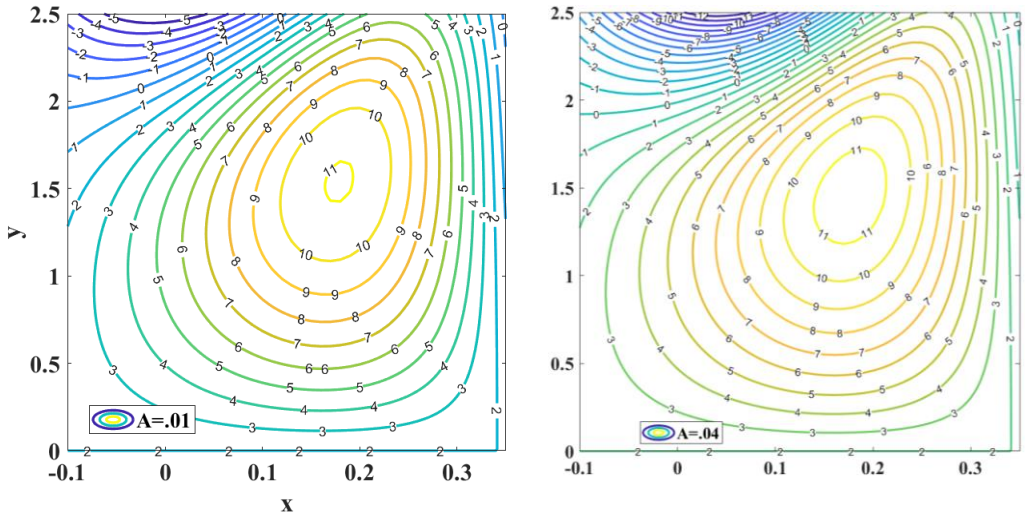

(a) (b)

Fig. 5. Effect of Eyring-Powell fluid parameter A on streamlines, with (a) A = 0.01, (b) A = 0.04

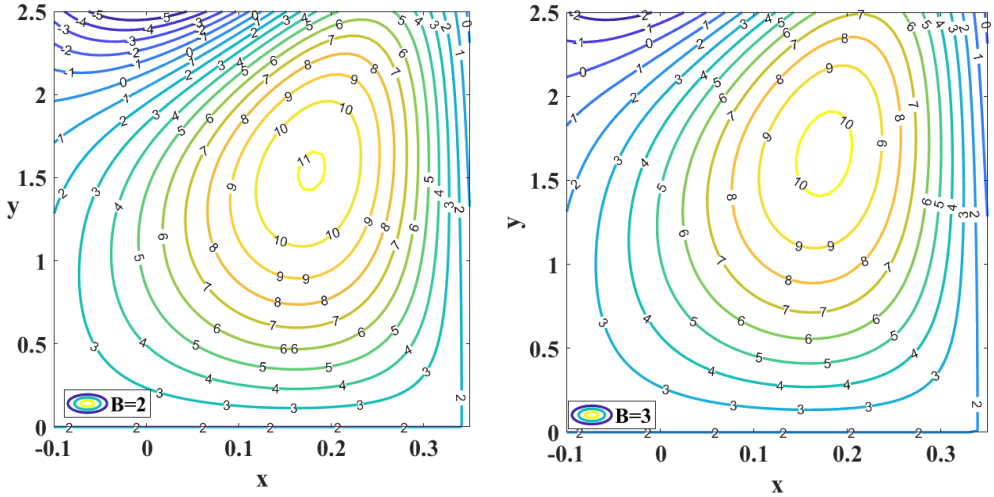

(a) (b)

Fig. 6. Effect of Eyring-Powell fluid parameter B on streamline profiles, when (a) B = 2, and (b) B = 3

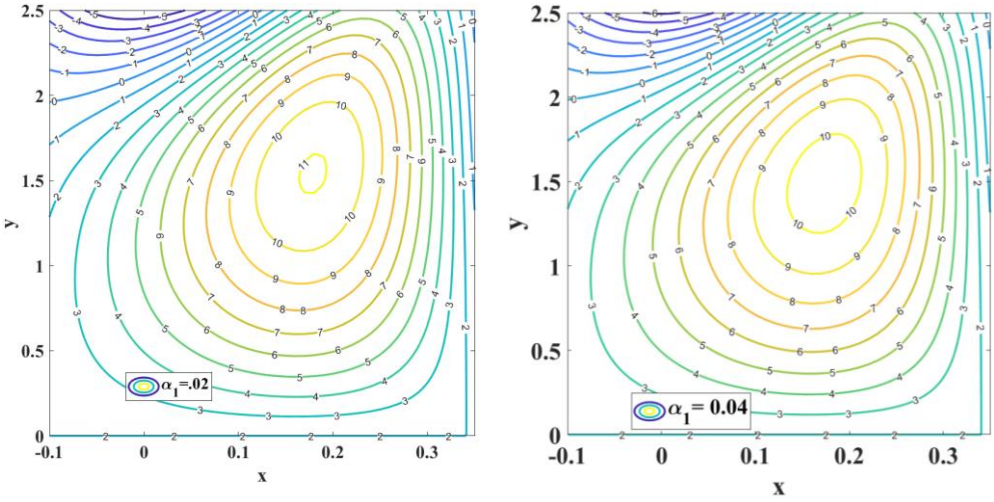

(a) (b)

Fig. 7. Effect of variable viscosity parameter (a) α_1= 0.02 and (b) α_1= 0.04

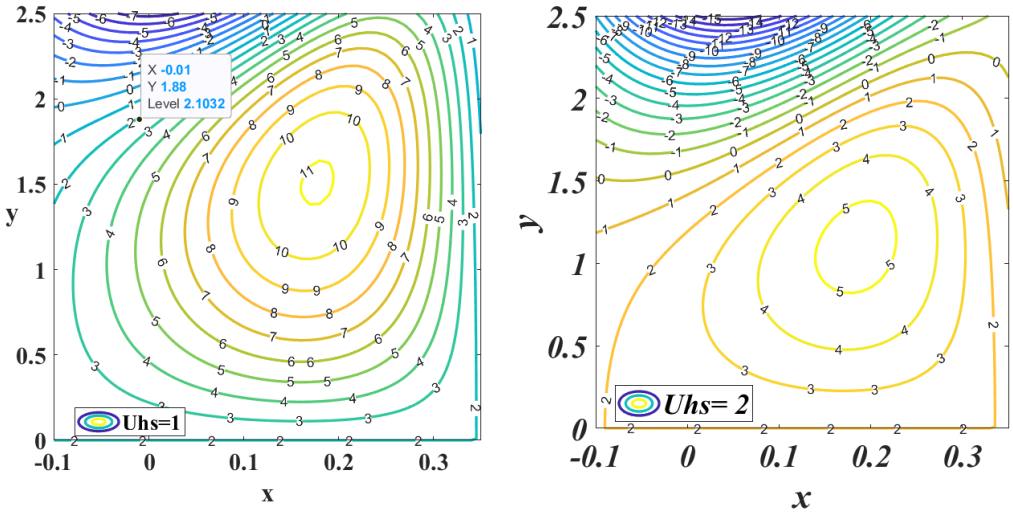

(a) (b)

Fig. 8. Effect of electroosmotic velocity on streamline profile, when (a) U_{hs}=1, and (b) U_{hs}=2

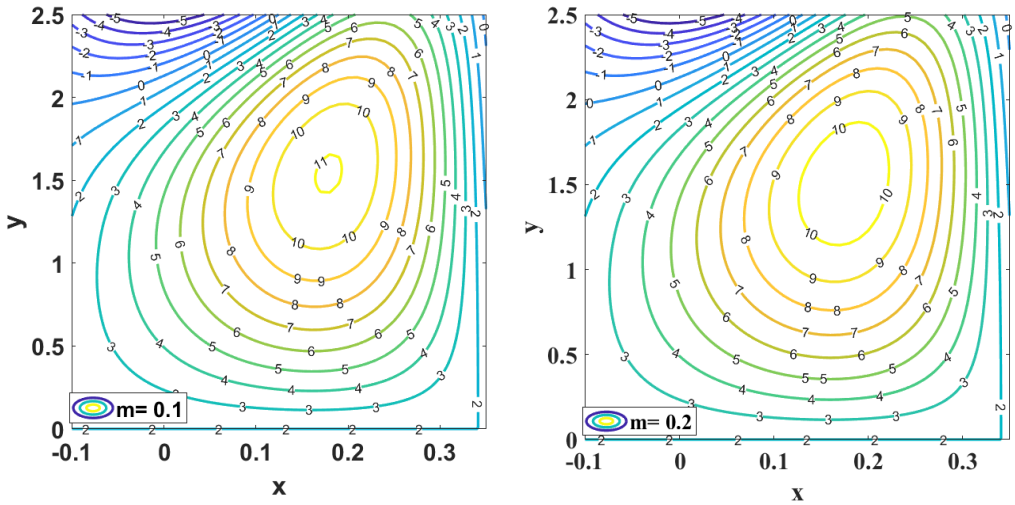

(a) (b)

Fig. 9. Effect of nonuniform parameter m on streamlines profiles, when (a) m = 0.1, and (b) m = 0.2

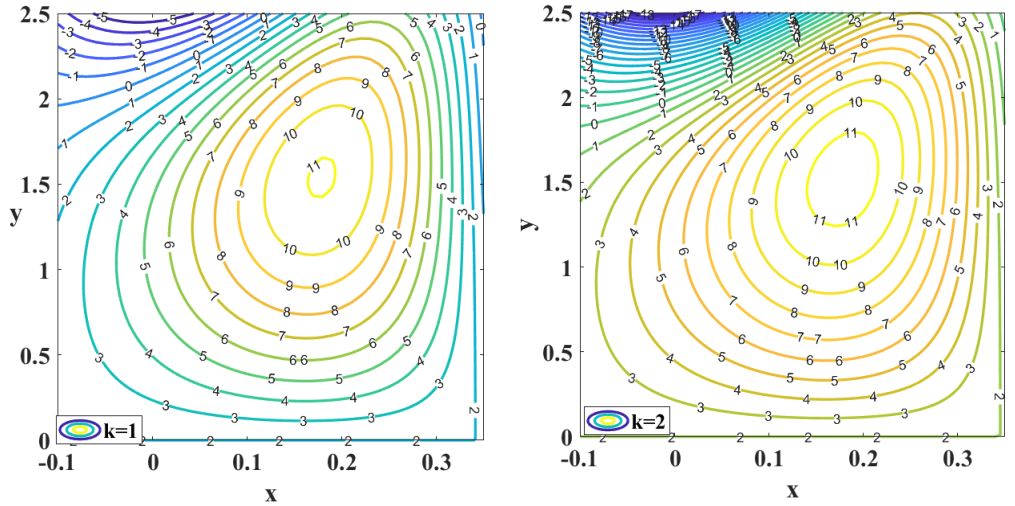

(a) (b)

Fig. 10. Effect of electroosmotic parameter k on streamlines profile, when (a) k=1, and (b) k=2

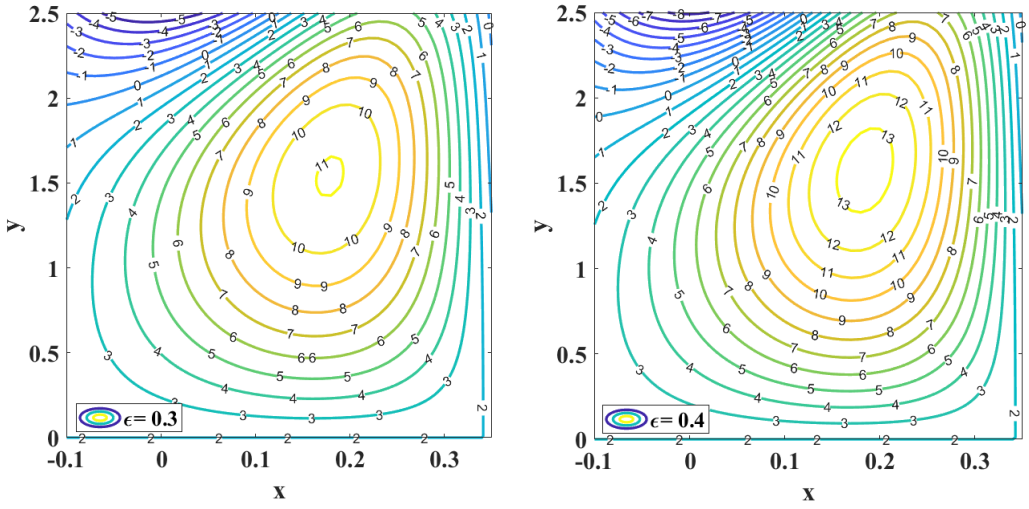

(a) (b)

Fig. 11. Effect of amplitude ratio ε on streamlines profile, with (a) $\varepsilon = 0.3$ and (b) ε =0.4

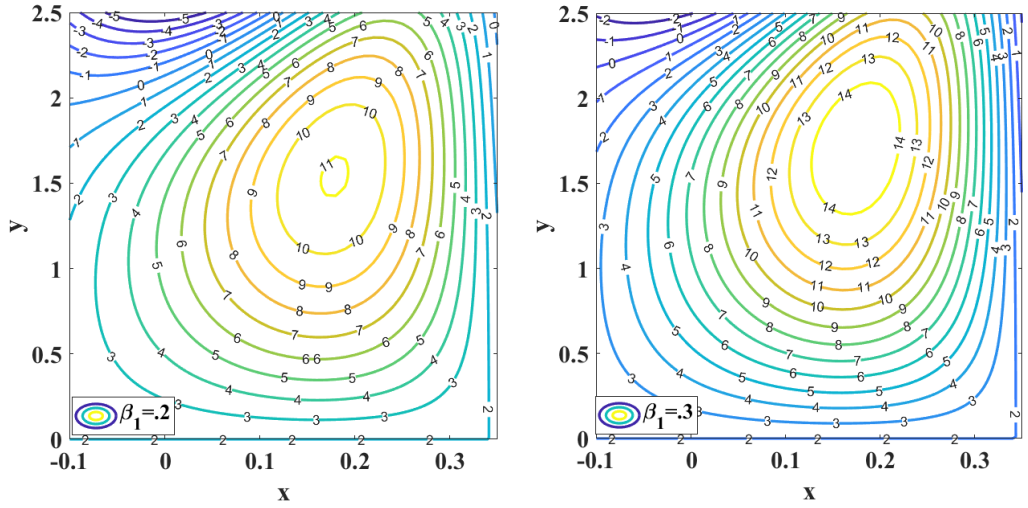

(a) (b)

Fig. 12. Effects of velocity slip parameter β_1 on streamlines profile, with (a) β_1 = 0.2 and (b) $\beta_1 = 0.3$

4. Conclusion

The Eyring-Powell fluid model has an electric field, slip, and fluctuating liquid properties as it passes through a non-uniform channel. The perturbation method is employed to solve the governing equations. Various factors affecting the flow in distinct profiles have been outlined. The results are applicable in the case of dysfunctional management of blood flow, also on considering peristaltic pumping mechanism, the role of viscosity and electroosmosis can be exploited. Some important findings from the model summarised as follows

i. The electroosmotic velocity and electroosmotic parameter, variable viscosity, material constant A and velocity slip parameters enhances the velocity profile, the material constant B, and wall damping coefficient diminishes velocity profile.
ii. The temperature is decreased by the Eyring-Powell model material constants parameters A and B and electroosmotic velocity, while the temperature profile is improved by the electroosmotic parameter, variable viscosity parameter, and amplitude ratio.

iii. The variable thermal conductivity, concentration slip parameter, material constant B and wall damping coefficient enhances and all other parameters diminishes the concentration profiles.
iv. Greater magnitude and lower number bolus occur for high electroosmotic velocity, velocity slip parameter and amplitude ratio increment result in higher number large magnitude boluses, the electroosmotic parameter k and material constant A increases the size of boluses, Material constant B, variable viscosity parameter, and nonuniform parameter diminishes the magnitude and number of the boluses slightly.

Acknowledgement
Research conducted without receiving any grants.

References
[1] Latham, Thomas Walker. "Fluid motions in a peristaltic pump." *PhD diss., Massachusetts Institute of Technology*, 1966.
[2] Shapiro, Ascher H., Michel Yves Jaffrin, and Steven Louis Weinberg. "Peristaltic pumping with long wavelengths at low Reynolds number." *Journal of Fluid Mechanics* 37, no. 4 (1969): 799-825. https://doi.org/10.1017/S0022112069000899
[3] Raju, K. Kanaka, and Rathna Devanathan. "Peristaltic motion of a non-Newtonian fluid." *Rheologica Acta* 11, no. 2 (1972): 170-178. https://doi.org/10.1007/BF01993016
[4] Srivastava, L. M., V. P. Srivastava, and S. N. Sinha. "Peristaltic transport of a physiological fluid." *Biorheology* 20, no. 2 (1983): 153-166. https://doi.org/10.3233/BIR-1983-20205
[5] Misra, J. C., and S. K. Pandey. "Peristaltic transport of a non-Newtonian fluid with a peripheral layer." *International Journal of Engineering Science* 37, no. 14 (1999): 1841-1858. https://doi.org/10.1016/S0020-7225(99)00005-1
[6] Hariharan, Prasanna, V. Seshadri, and Rupak K. Banerjee. "Peristaltic transport of non-Newtonian fluid in a diverging tube with different wave forms." *Mathematical and Computer Modelling* 48, no. 7-8 (2008): 998-1017. https://doi.org/10.1016/j.mcm.2007.10.018
[7] Ellahi, R., M. Mubashir Bhatti, and K. Vafai. "Effects of heat and mass transfer on peristaltic flow in a non-uniform rectangular duct." *International Journal of Heat and Mass Transfer* 71 (2014): 706-719. https://doi.org/10.1016/j.ijheatmasstransfer.2013.12.038
[8] Akram, Safia, S. Nadeem, and Anwar Hussain. "Effects of heat and mass transfer on peristaltic flow of a Bingham fluid in the presence of inclined magnetic field and channel with different wave forms." *Journal of Magnetism and Magnetic Materials* 362 (2014): 184-192. https://doi.org/10.1016/j.jmmm.2014.02.063
[9] Saleem, Musharafa, and Aun Haider. "Heat and mass transfer on the peristaltic transport of non-Newtonian fluid with creeping flow." *International Journal of Heat and Mass Transfer* 68 (2014): 514-526. https://doi.org/10.1016/j.ijheatmasstransfer.2013.09.053
[10] Bhatti, M. M., A. Zeeshan, R. Ellahi, and G. C. Shit. "Mathematical modeling of heat and mass transfer effects on MHD peristaltic propulsion of two-phase flow through a Darcy-Brinkman-Forchheimer porous medium." *Advanced Powder Technology* 29, no. 5 (2018): 1189-1197. https://doi.org/10.1016/j.apt.2018.02.010
[11] Hosham, Hany A., and N. M. Hafez. "Bifurcation phenomena in the peristaltic transport of non-Newtonian fluid with heat and mass transfer effects." *Journal of Applied Mathematics and Computing* 67, no. 1 (2021): 275-299. https://doi.org/10.1007/s12190-020-01477-7
[12] El-Shehawy, E. F., N. T. El-Dabe, and I. M. El-Desoky. "Slip effects on the peristaltic flow of a non-Newtonian Maxwellian fluid." *Acta Mechanica* 186 (2006): 141-159. https://doi.org/10.1007/s00707-006-0343-6
[13] Abumandour, Ramzy M., I. M. Eldesoky, and Faisal A. Kroush. "Effects of slip conditions and compressibility on the peristaltic flow of particulate suspension in a planar channel." *SN Applied Sciences* 1 (2019): 1305. https://doi.org/10.1007/s42452-019-1309-3
[14] Vajravelu, K., S. Sreenadh, and R. Saravana. "Combined influence of velocity slip, temperature and concentration jump conditions on MHD peristaltic transport of a Carreau fluid in a non-uniform channel." *Applied Mathematics and Computation* 225 (2013): 656-676. https://doi.org/10.1016/j.amc.2013.10.014
[15] Kamel, Mohammed H., Islam M. Eldesoky, Bilal M. Maher, and Ramzy M. Abumandour. "Slip effects on peristaltic transport of a particle-fluid suspension in a planar channel." *Applied Bionics and Biomechanics* 2015, no. 1 (2015): 703574. https://doi.org/10.1155/2015/703574
[16] Vaidya, Hanumesh, Oluwole Daniel Makinde, Rajashekhar Choudhari, Kerehalli Vinayaka Prasad, Sami Ullah Khan, and Kuppalapalle Vajravelu. "Peristaltic flow of non-Newtonian fluid through an inclined complaint nonlinear tube:

application to chyme transport in the gastrointestinal tract." *European Physical Journal Plus* 135, no. 11 (2020): 934. https://doi.org/10.1140/epjp/s13360-020-00899-3

[17] Ibrahim, M. G., and M. Y. Abou-Zeid. "Influence of variable velocity slip condition and activation energy on MHD peristaltic flow of Prandtl nanofluid through a non-uniform channel." *Scientific Reports* 12, no. 1 (2022): 18747. https://doi.org/10.1038/s41598-022-23308-4

[18] Khan, Ambreen Afsar, Rahmat Ellahi, and Muhammad Usman. "The effects of variable viscosity on the peristaltic flow of non-Newtonian fluid through a porous medium in an inclined channel with slip boundary conditions." *Journal of Porous Media* 16, no. 1 (2013). https://doi.org/10.1615/JPorMedia.v16.i1.60

[19] Vaidya, Hanumesh, Rajashekhar Choudhari, Manjunatha Gudekote, and Kerehalli Vinayaka Prasad. "Effect of variable liquid properties on peristaltic transport of Rabinowitsch liquid in convectively heated complaint porous channel." *Journal of Central South University* 26, no. 5 (2019): 1116-1132. https://doi.org/10.1007/s11771-019-4075-x

[20] Choudhari, Rajashekhar, Hanumesh Vaidya, Kerehalli Vinayaka Prasad, Manjunatha Gudekote, M. Ijaz Khan, Mehdi Akermi, Rym Hassani, Hala A. Hejazi, and Shahid Ali. "Analysis of peristalsis blood flow mechanism using non-newtonian fluid and variable liquid characteristics." *Results in Engineering* 21 (2024): 101842. https://doi.org/10.1016/j.rineng.2024.101842

[21] Balachandra, H., Choudhari Rajashekhar, Hanumesh Vaidya, Fateh Mebarek Oudina, Gudekote Manjunatha, Kerehalli Vinayaka Prasad, and Prathiksha Prathiksha. "Homogeneous and heterogeneous reactions on the peristalsis of bingham fluid with variable fluid properties through a porous channel." *Journal of Advanced Research in Fluid Mechanics and Thermal Sciences* 88, no. 3 (2021): 1-19. https://doi.org/10.37934/arfmts.88.3.119

[22] Vaidya, Hanumesh, Kerehalli Vinayaka Prasad, Rajashekhar Choudhari, Shivaleela Shivaleela, Shivaraya Keriyappa, Manjunatha Gudekote, and Jyoti Shetty. "Partial slip effects on MHD peristaltic flow of Carreau-Yasuda fluid (CY) through a planner micro-channel." *Journal of Advanced Research in Fluid Mechanics and Thermal Sciences* 104, no. 2 (2023): 65-85. https://doi.org/10.37934/arfmts.104.2.6585

[23] Basha, Neelufer Z., F. Mebarek-Oudina, Rajashekhar Choudhari, Hanumesh Vaidya, Balachandra Hadimani, K. V. Prasad, Manjunatha Gudekote, and Sangeeta Kalal. "Thermal Radiation Effect on Mixed Convective Casson Fluid Flow over a Porous Stretching Sheet with Variable Fluid Properties." *Journal of Advanced Research in Fluid Mechanics and Thermal Sciences* 111, no. 1 (2023): 1-27. https://doi.org/10.37934/arfmts.111.1.127

[24] Akbar, Noreen Sher, Abbasali Abouei Mehrizi, Maimona Rafiq, M. Bilal Habib, and Taseer Muhammad. "Peristaltic flow analysis of thermal engineering nano model with effective thermal conductivity of different shape nanomaterials assessing variable fluid properties." *Alexandria Engineering Journal* 81 (2023): 395-404. https://doi.org/10.1016/j.aej.2023.09.027

[25] Das, Siddhartha, and Suman Chakraborty. "Analytical solutions for velocity, temperature and concentration distribution in electroosmotic microchannel flows of a non-Newtonian bio-fluid." *Analytica Chimica Acta* 559, no. 1 (2006): 15-24. https://doi.org/10.1016/j.aca.2005.11.046

[26] Ranjit, N. K., and G. C. Shit. "Entropy generation on electro-osmotic flow pumping by a uniform peristaltic wave under magnetic environment." *Energy* 128 (2017): 649-660. https://doi.org/10.1016/j.energy.2017.04.035

[27] Noreen, Saima, Sadia Waheed, Abid Hussanan, and Dianchen Lu. "Analytical solution for heat transfer in electroosmotic flow of a Carreau fluid in a wavy microchannel." *Applied Sciences* 9, no. 20 (2019): 4359. https://doi.org/10.3390/app9204359

[28] Saleem, Salman, Salman Akhtar, Sohail Nadeem, Anber Saleem, Mehdi Ghalambaz, and Alibek Issakhov. "Mathematical study of electroosmotically driven peristaltic flow of Casson fluid inside a tube having systematically contracting and relaxing sinusoidal heated walls." *Chinese Journal of Physics* 71 (2021): 300-311. https://doi.org/10.1016/j.cjph.2021.02.015

[29] Tanveer, Anum, Sidra Mahmood, Tasawar Hayat, and Ahmed Alsaedi. "On electroosmosis in peristaltic activity of MHD non-Newtonian fluid." *Alexandria Engineering Journal* 60, no. 3 (2021): 3369-3377. https://doi.org/10.1016/j.aej.2020.12.051

[30] Choudhari, Rajashekhar, Fateh Mebarek-Oudina, Hakan F. Öztop, Hanumesh Vaidya, and Kerehalli Vinayaka Prasad. "Electro-osmosis modulated peristaltic flow of non-Newtonian liquid via a microchannel and variable liquid properties." *Indian Journal of Physics* 96, no. 13 (2022): 3853-3866. https://doi.org/10.1007/s12648-022-02326-y

[31] Akram, Javaria, and Noreen Sher Akbar. "Electroosmotically actuated peristaltic-ciliary flow of propylene glycol+ water conveying titania nanoparticles." *Scientific Reports* 13, no. 1 (2023): 11801. https://doi.org/10.1038/s41598-023-38820-4

[32] Akbar, Noreen Sher, and Taseer Muhammad. "Physical aspects of electro osmotically interactive Cilia propulsion on symmetric plus asymmetric conduit flow of couple stress fluid with thermal radiation and heat transfer." *Scientific Reports* 13, no. 1 (2023): 18491. https://doi.org/10.1038/s41598-023-45595-1

[33] Akbar, Noreen Sher, Maimona Rafiq, Taseer Muhammad, and Metib Alghamdi. "Electro osmotically interactive biological study of thermally stratified micropolar nanofluid flow for Copper and Silver nanoparticles in a microchannel." *Scientific Reports* 14, no. 1 (2024): 518. https://doi.org/10.1038/s41598-023-51017-z

[34] Akbar, Noreen Sher, and S. Nadeem. "Characteristics of heating scheme and mass transfer on the peristaltic flow for an Eyring-Powell fluid in an endoscope." *International Journal of Heat and Mass Transfer* 55, no. 1-3 (2012): 375-383. https://doi.org/10.1016/j.ijheatmasstransfer.2011.09.029

[35] Noreen, S., and M. Qasim. "Peristaltic flow of MHD Eyring-Powell fluid in a channel." *The European Physical Journal Plus* 128 (2013): 91. https://doi.org/10.1140/epjp/i2013-13091-3

[36] Abbasi, F. M., A. Alsaedi, and T. Hayat. "Peristaltic transport of Eyring-Powell fluid in a curved channel." *Journal of Aerospace Engineering* 27, no. 6 (2014): 04014037. https://doi.org/10.1061/(ASCE)AS.1943-5525.0000354

[37] Hina, S. "MHD peristaltic transport of Eyring-Powell fluid with heat/mass transfer, wall properties and slip conditions." *Journal of Magnetism and Magnetic Materials* 404 (2016): 148-158. https://doi.org/10.1016/j.jmmm.2015.11.059

[38] Bhattacharyya, A., R. Kumar, S. Bahadur, and G. S. Seth. "Modeling and interpretation of peristaltic transport of Eyring-Powell fluid through uniform/non-uniform channel with Joule heating and wall flexibility." *Chinese Journal of Physics* 80 (2022): 167-182. https://doi.org/10.1016/j.cjph.2022.06.018

[39] Rehman, Khalil Ur, Wasfi Shatanawi, and M. Y. Malik. "Group theoretic thermal analysis (GTTA) of Powell-Eyring fluid flow with Identical free stream (FS) and heated stretched porous (HSP) boundaries: AI Decisions." *Case Studies in Thermal Engineering* 55 (2024): 104101. https://doi.org/10.1016/j.csite.2024.104101

[40] Rehman, Khalil Ur, and Wasfi Shatanawi. "Lie symmetry based neural networking analysis for Powell-Eyring fluid flow with heat and mass transfer effects." *International Journal of Thermofluids* 22 (2024): 100602. https://doi.org/10.1016/j.ijft.2024.100602

[41] Akbar, Noreen Sher, and S. Nadeem. "Characteristics of heating scheme and mass transfer on the peristaltic flow for an Eyring-Powell fluid in an endoscope." *International Journal of Heat and Mass Transfer* 55, no. 1-3 (2012): 375-383. https://doi.org/10.1016/j.ijheatmasstransfer.2011.09.029

[42] Gudekote, Manjunatha, Rajashekhar Choudhari, Prathiksha Sanil, Hanumesh Vaidya, Balachandra Hadimani, Kerehalli Vinayaka Prasad, and Jyoti Shetty. "Impact of Variable Liquid Properties on Peristaltic Transport of Non-Newtonian Fluid Through a Complaint Non-Uniform Channel." *Journal of Advanced Research in Fluid Mechanics and Thermal Sciences* 103, no. 2 (2023): 20-39. https://doi.org/10.37934/arfmts.103.2.2039